Hollow copper microneedle made by local electrodeposition-based additive manufacturing

Roger Sachan[1], Patrik Schürch[2], Paolo Testa[2], Edgar Hepp[2], Wabe W. Koelmans[2], Roger J. Narayan[3]

[1]Department of Biochemistry, North Carolina State University, Raleigh, NC 27695

[2] Exaddon AG, Sägereistrasse 25, 8152 Zürich, Switzerland

[3] Joint Department of Biomedical Engineering, University of North Carolina, Chapel Hill, NC USA 27599; rjnaraya@ncsu.edu

* Correspondence; rjnaraya@ncsu.edu

Abstract

Additive manufacturing offers the opportunity to manufacture microscale devices with custom designs such as microneedles, which have potential use in the transdermal delivery of vaccines or drugs. In this paper, a hollow microneedle was created out of copper using a local electrodeposition-based additive manufacturing processing. Scanning electron microscopy and confocal laser scanning microscopy revealed that the microneedle contained a sharp tip and a hollow bore. X-ray photoelectron spectroscopy showed the presence of copper, oxygen, copper, silicon, and sulfur and the absence of toxic impurities in a solid microneedle. These results suggest that local electrodeposition-based additive manufacturing of copper may be an appropriate approach for producing microneedles and many other types of microscale medical devices.

Introduction

Copper has several useful properties that make it useful for manufacturing medical devices; most significantly, it is widely available at low cost [1]. Since it is a weak sensitizer in comparison to other metals, copper is used in jewelry and wearable products [2, 3]. In addition, copper is used in medical products such as dental amalgam and intrauterine devices; for example, copper intrauterine devices can be used safely in the body for at least five years [4, 5].

In this study, we consider the use of an additive manufacturing approach based on local electrodeposition to create a copper microneedle. This approach is associated with several benefits, including a large degree of design freedom, the capability for template-free rapid prototyping of structures, and the capability for rapid manufacturing in support of low volume production applications. Hollow microneedles are small-scale needle-shaped devices that are used to penetrate the skin for the delivery of vaccines or drugs through the skin [6]. Although Gerstel and Place described the use of microneedles-based drug delivery in 1976, significant efforts to translate microneedle technology have only taken place in the past two decades [7, 8]. The delivery of a vaccine or drug using hollow microneedles involves a “poke and flow” process, in which there is movement of a vaccine or drug through a hollow microneedle via diffusion or effusion from the device through the skin [8]. The microstructure of the copper microneedle was characterized via scanning electron microcopy and confocal laser scanning microscopy; X-ray photoelectron spectroscopy was used to understand the chemical composition of the hollow microneedle. The results of this study show the promise of local electrodeposition-based additive manufacturing for manufacturing microscale medical devices such as microneedles.

Experimental Procedure

The microneedles were made using an additive micromanufacturing (µAM) approach that is based on local electrodeposition [9]. This approach, as utilized in the CERES system (Exaddon AG, Zürich, Switzerland), involves a combination of fluidic scanning probes and 3D printing (Figure 1). A cantilever holding a microfluidic channel and a hollow tip is submerged in a three-electrode electrochemical cell (Figure 2). A $CuSO_4$ solution is released into the cell by the tip; air pressure expels the $CuSO_4$ solution from the tip. This localized ion supply confines the electrochemical reduction to a small region at the working electrode. Using this approach, a unit building block, also known as a voxel (volumetric pixel), is formed.

In the first step, the hollow tip with an aperture of 300 nm in diameter (Iontip, Exaddon AG, Zürich, Switzerland) is maintained at a selected separation, which equals the voxel height, from the working electrode. The magnitude of the air pressure determines the lateral size of the voxel [10]. In a second step, the copper metal deposits until the tip is reached. When the voxel touches the tip, the cantilever deflects upwards. The cantilever motion is detected using an optical beam deflection system. When the voxel is completed, the tip moves to the next voxel coordinate. The microneedle was processed using 42,682 voxels; the printing time was approximately 6 hours. The microneedle manufacturing process was performed with an air pressure of 60 mbar applied to the reservoir feeding the iontip.

After the additive micromanufacturing procedure, a conformal, non-local, copper plating procedure was carried out on the microneedle. In the three-electrode setup, the microneedle was used as a working electrode, a platinum wire was used as a counter electrode, and

Ag/AgCl was used as a reference electrode. The microneedle is contacted by the substrate surface, which, in turn, is contacted by graphite electrodes to the working electrode of the potentiostat. The 0.5M $CuSO_4$ * $5H_2O$ (98%, Sigma Aldrich) solution used for copper plating was adjusted to a pH of 3.00 with 0.1 M sulfuric acid. The deposition took place for 30 seconds; an applied potential of -0.50V vs Ag/AgCl and a average current of 2-3 mA/cm^2 were used for plating.

Scanning electron microscopy was performed with a Sigma microscope (Carl Zeiss AG, Oberkochen, Germany) using an acceleration voltage of 12kV and a current of 10 μA. Imaging was not corrected for the tilt. The microneedle morphology and height were evaluated using a VKx1100 confocal laser scanning microscope (Keyence, Osaka, Japan). A SPECS X-ray photoelectron spectroscopy containing a PHOIBOS 150 Hemispherical Analyzer (SPECS Surface Nano Analysis GmbH, Berlin, Germany) was used to obtain elemental composition data from the microneedle.

Results and Discussion

Figure 3 shows a scanning electron micrograph of a hollow copper microneedle taken at a 45° angle tilt. Confocal laser scanning microscopy has been previously used to understand topographical features of microneedles [11]. Figure 4 contains confocal laser scanning micrographs of a hollow copper microneedle; Figure 4 (a) shows an optical micrograph of the hollow copper microneedle in the top-down orientation, and Figure 4 (b) shows a 3D representation of the hollow copper microneedle. The needle shows a sharp tip; in addition, needle bore was shown to be hollow from optical imaging of the needle in the top-down orientation. Confocal laser scanning microscopy showed that the height of the microneedle was 431 μm; this value is close to the height of the design (400 μm) that was used for additive manufacturing of the microneedle. The microstructural features of the hollow microneedle (e.g., the sharpness of the microneedle tip) appear to be appropriate for transdermal delivery of vaccines or drugs.

Figure 5 shows an X-ray photoelectron spectrum from a solid copper microneedle (i.e., a microneedle with a closed bore). The survey scan showed that the microneedle contained copper, oxygen, copper, silicon, and sulfur. The copper peak is consistent with the presence of CuO. The presence of oxygen was attributed to CuO, which forms on the surface of the copper structure in air, and oxygen in the print ink. The presence of carbon was attributed to the additives within the copper print ink and to the graphite electrodes used in the additive manufacturing process. Curve fitting of the silicon peak showed that the silicon, which was attributed to residues within the chamber (as standard substrates used in the additive manufacturing process are made of silicon) contained two components; the peak at a higher binding energy was attributed to SiO_2 and the peak at a lower binding energy was attributed to elemental silicon [12, 13]. The sulfur in the spectrum was attributed to its presence in the printing ink. No other elements, particularly elements of known toxicity, were noted in the spectrum. This composition of the microneedle appears to be appropriate for transient contact with the skin. The impurities can be eliminated by either not using additives or non-carbon based additives during printing. Also, a non-carbon electrode material, such as gold or platinum, may be used.

Conclusions

A hollow microneedle was made from copper using a local electrodeposition-based additive manufacturing approach. Confocal laser scanning microscopy and scanning electron microscopy showed that the microneedle exhibited a sharp tip, a hollow bore, and a height measurement that was similar to that of the computer design that was used to manufacture the microneedle. X-ray photoelectron spectroscopy revealed the presence of copper, oxygen, copper, silicon, and sulfur and as well as the absence of toxic impurities in a solid microneedle; the impurities in the copper microneedle were attributed to the materials used in the local electrodeposition-based additive manufacturing process. These results suggest that the local electrodeposition-based additive manufacturing of copper may be used to manufacture microneedles and a variety of customized microscale medical devices.

Conflict of Interest Statement

Patrik Schürch, Paolo Testa, Edgar Hepp, and Wabe W. Koelmans are affiliated with Exaddon AG, which has developed the technology that is described in this study. Roger Sachan and Roger J. Narayan have no conflicts of interest.

Data Availability Statement

The datasets generated during and/or analyzed during the current study are available from the corresponding author on reasonable request.

References

1. N. Thokala, C. Kealey, J. Kennedy, D. B. Brady, and J. B. Farrell, Materials Science and Engineering: C, 78, 1179-1186 (2017).

2. S.W. Fage, A. Faurschou, and J.P. Thyssen, Contact Dermatitis, 71, 191-201, 2014.

3. P. Li, Y. Zhao, J. Ma, Y. Yang, H. Xu, and Y. Liu, Advanced Materials Technologies, 5, 1900823, 2020.

4. D. R. Beech, International Dental Journal, 32, 240-251, 1982.

5. J. Newton and D. Tacchi, Lancet, 335, 1322-1323, 1990.

6. R. J. Narayan, Journal of Biomedical Nanotechnology, 10, 2244-2260, 2014.

7. M.S. Gerstel and V.A. Place, Drug delivery device. US Patent No. 3964482, 1976.

8. S. H. Bariya, M. C. Gohel, T.A. Mehta, and O.P. Sharma, Journal of Pharmacy and Pharmacology, 64, 11-29, 2012.

9. G. Ercolano, T. Zambelli, C. van Nisselroy, D. Momotenko, J. Vörös, T. Merle, and W.W. Koelmans, Advanced Engineering Materials, 22, 1900961, 2020.

10. G. Ercolano, C. van Nisselroy, T. Merle, J. Vörös, D. Momotenko, W.W. Koelmans, and T. Zambelli, Micromachines, 11, 6, 2020.

11. A. Sachan, R.J. Sachan, J. Lu, H. Sun, Y.J. Jin, D. Erdmann, J.Y. Zhang, and R.J. Narayan, MRS Advances, 6, 61-65, 2021.

12. J. A. Tossell, D. J. Vaughan, and K. H. Johnson, Chemical Physics Letters, 20, 329-334 (1973).

13. Y. Tao, Z. H. Lu, M. J. Graham, and S. P. Tay, Journal of Vacuum Science & Technology B, 12, 2500-3 (1994).

Figure Captions

Figure 1. Schematic of the CERES system that was used for additive manufacturing of the structures. The system computer on the left provides commands to the positioning control module on the right. The positioning control module regulates the additive manufacturing process via an embedded controller. The hollow cantilever, which is located on the printing head, is moved using the z-stage in the printing chamber. The microfluidics control system modulates the electrolyte flow via the cantilever aperture. Adapted with permission from [9].

Figure 2. Schematic of the printing process, which shows copper ions being locally injected through the cantilever aperture in the printing chamber; this process occurs in proximity (500 nm) of the growing microneedle (WE). On the metal surface, the ions are electrochemically reduced to copper; this process forms the printed voxel. When the reduction front reaches the cantilever, it is deflected (optical beam deflection); this process automatically triggers positioning to the next location. The terms WE, CE, and RE refer to the working electrode, counter electrode, and reference electrode, respectively. Adapted with permission from [9].

Figure 3. Scanning electron micrograph of a hollow copper microneedle taken at a 45° angle tilt.

Figure 4. Confocal laser scanning micrograph of a hollow copper microneedle. (a) An optical micrograph of the hollow copper microneedle in the top-down orientation. (b) A 3D representation of the hollow copper microneedle.

Figure 5. X-ray photoelectron spectrum from a solid copper microneedle.

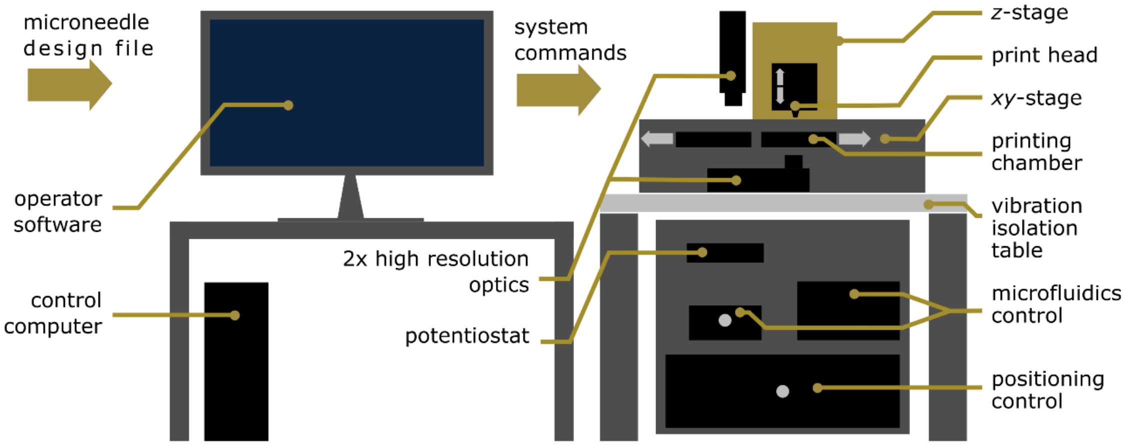
microneedle
design file
system
commands
operator
software
control
computer
2x high resolution
optics
potentiostat
z-stage
print head
xy-stage
printing
chamber
vibration
isolation
table
microfluidics
control
positioning
control

Figure 1.

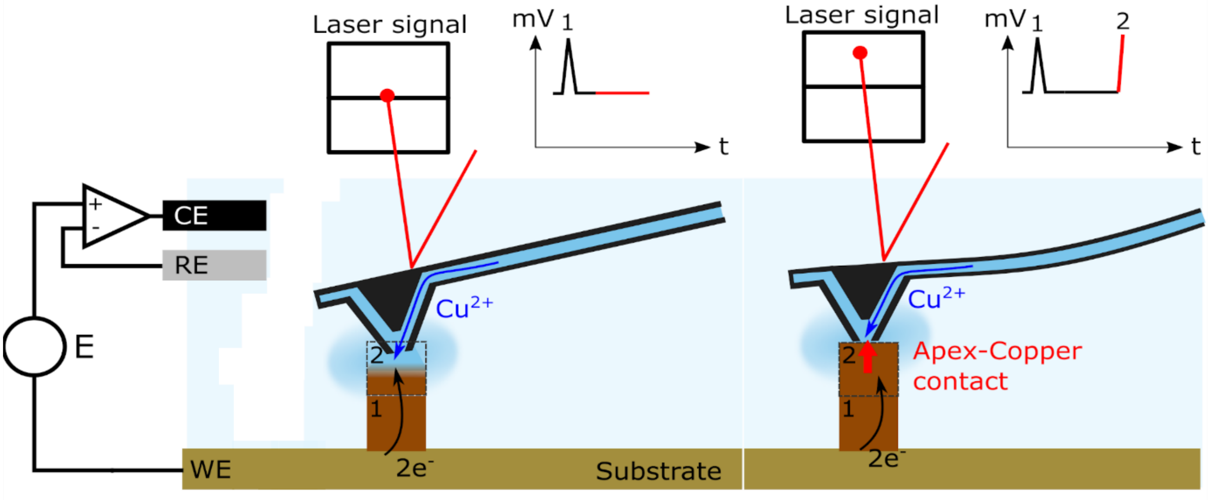
Laser signal
mV
1
t
Laser signal
mV
1
2
t
+
-
CE
RE
E
Cu2+
2
1
2e-
Cu2+
2
1
Apex-Copper
contact
2e-
WE
Substrate

Figure 2.

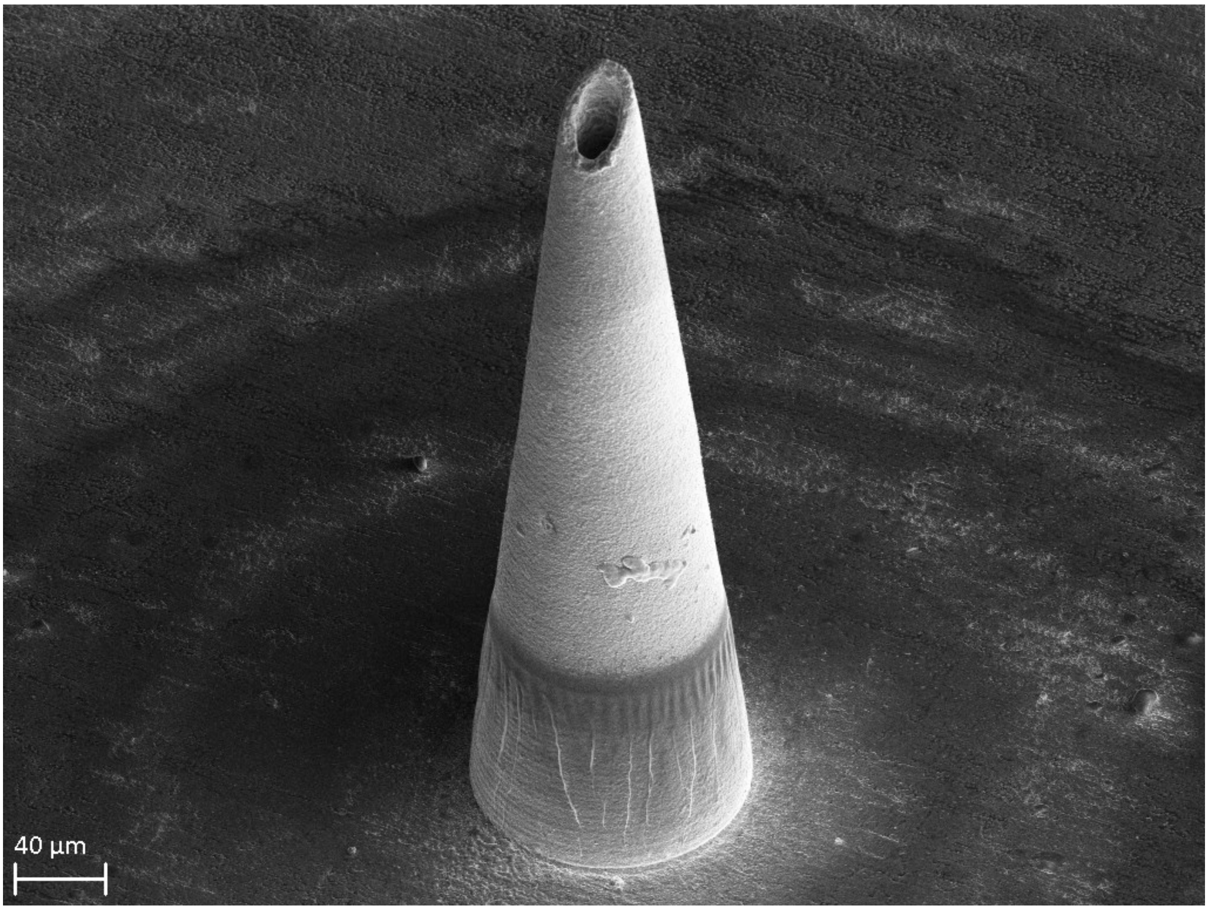

Figure 3.

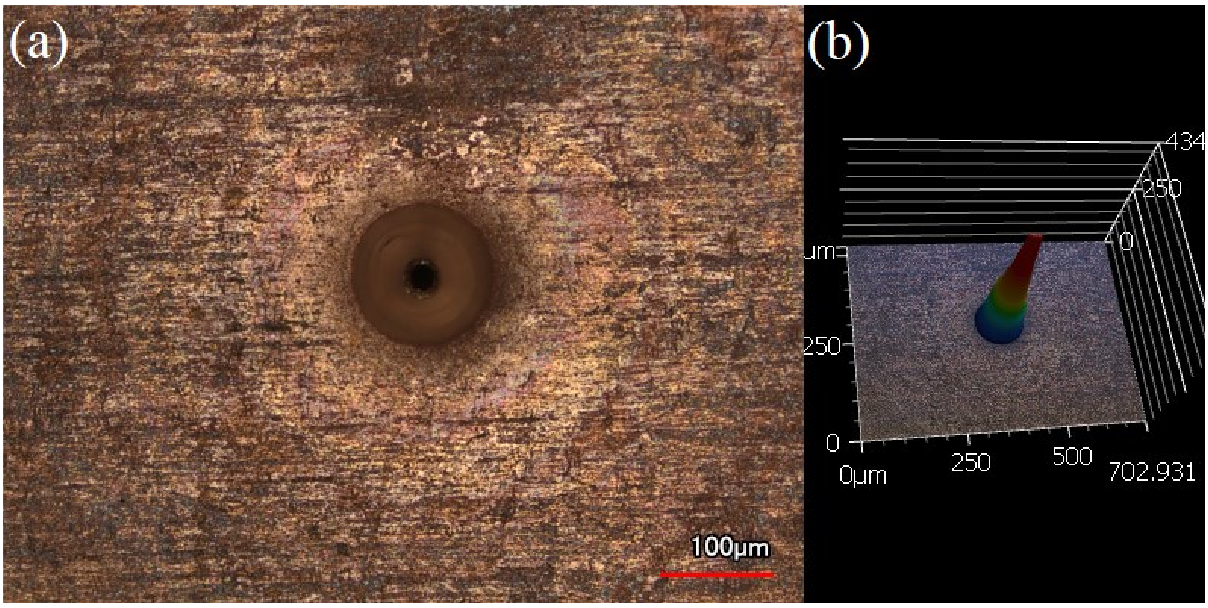

Figure 4.

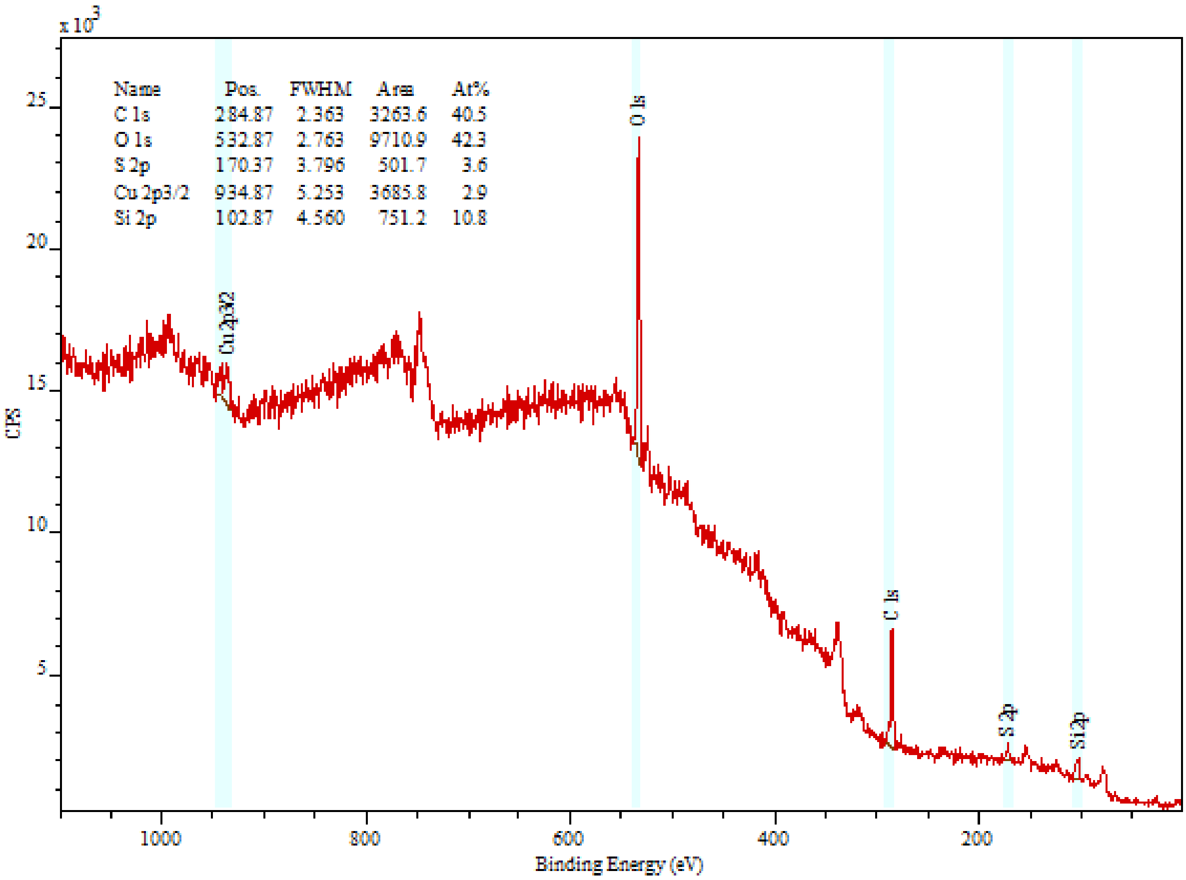
x 10^3
Name Pos. FWHM Area At%
C 1s 284.87 2.363 3263.6 40.5
O 1s 532.87 2.763 9710.9 42.3
S 2p 170.37 3.796 501.7 3.6
Cu 2p3/2 934.87 5.253 3685.8 2.9
Si 2p 102.87 4.560 751.2 10.8
O 1s
Cu 2p3/2
C 1s
S 2p
Si 2p
CPS
25
20
15
10
5
1000
800
600
400
200
Binding Energy (eV)

Figure 5.